Energy Strategy Reviews 44 (2022) 100974

Contents lists available at ScienceDirect

Energy Strategy Reviews

journal homepage: www.elsevier.com/locate/esr

Minigrid integration planning (MGIP) for loss reduction and voltage profile improvement beyond energy access in developing countries

Madalitso Chikumbanje *, Damien Frame, Stuart Galloway

Department of Electronic and Electrical Engineering, University of Strathclyde, Glasgow, UK

ARTICLE INFO

Keywords:
Energy access
Minigrids
Network expansion
Grid integration
Optimization
Sustainable development goal 7 (SDG7)

ABSTRACT

To improve access to electricity and achieve Sustainable Development Goal 7 (SDG7), a mixture of grid extension and off-grid systems, like minigrids, are under deployment in many developing countries, including sub-Saharan Africa (SSA). Beyond meeting energy access goals, the main grid will continue expanding and eventually converge and integrate with minigrids. Such integration has the potential to address network losses and low quality of supply in developing countries, similar to how the optimal placement and sizing of distributed energy resources (DERs) has impacted distribution networks in the global north. However, unlike in the DER integration, there is no suitable planning methodology for maximizing the benefits of grid integration of formerly autonomous minigrids in developing countries. This paper proposes a minigrid integration planning (MGIP) methodology that ensures loss reduction and voltage improvement in post-energy access networks in developing countries. The planning problem is formulated as a mixed-integer non-linear problem (MINLP) and is solved using a Genetic Algorithm (GA). The paper demonstrates MGIP's ability to ensure loss reduction and voltage profile improvement by identifying optimal points of grid infeed into formerly autonomous minigrids. It also shows MGIP's flexibility to be applicable in a basic case of integrating a single minigrid and an advanced case of integrating a cluster of minigrids. The results show that using the MGIP approach can significantly reduce losses (by up to 65% as observed in some scenarios of the reported case studies) and improve voltage profile through the grid integration of formerly autonomous minigrids in the post-SDG7 electrical networks in developing countries.

Author contributions

Madalitso Chikumbanje: Conceptualization, Formal analysis, Investigation, Methodology, Writing – original draft; **Damien Frame**: Supervision, Writing – review & editing, Validation; **Stuart Galloway**: Supervision, Writing – review & editing, Resources, Methodology

1. Introduction

Achieving access to affordable, reliable, and modern energy services for all by 2030 is one of the primary objectives under the United Nations' Sustainable Development Goal 7 (SDG7) [1]. Pathways for meeting this goal in developing countries by 2030 include grid expansion and various off-grid energy access interventions such as minigrids and Solar Home Systems (SHS) [2]. Although current projections in Ref. [3] suggest that the 2030 target may be over-ambitious, there is considerable progress towards achieving SDG7. On this progress, Tracking SDG7 2021 report [3] highlights a 30% reduction in people without access to electricity, from 1.2 billion in 2010 to 759 million in 2019. This reduction is significant because demographics may diminish its extent as regions with electricity access challenges, like sub-Saharan Africa (SSA), are also synonymous with high population growth rates [2].

While there is steady progress in achieving electricity access, SSA continues to be associated with high electricity network losses [4,5], low quality of service [6], and poor reliability of supply [7,8]. Recognizing the variation in quality and reliability of electricity access initiatives, the World Bank introduced a five tier classification of electricity access called the Multi-Tier Framework (MTF) [9], where Tier 1 access translates to an annual energy consumption of around 4.5 kWh compared to over 3,000 kWh for Tier 5 access [10]. Offgrid systems for energy access supply Tier 3 access or lower [8]. While higher tiers of access should be expected from national grids, many SSA grids are already struggling to meet demand with the available installed generation capacities and high losses (averaging 16% compared to 9% in other developing countries) exacerbate the problem [2]. Therefore, addressing these other

* Corresponding author.
E-mail addresses: madalitso.chikumbanje@strath.ac.uk (M. Chikumbanje), damien.frame@strath.ac.uk (D. Frame), stuart.galloway@strath.ac.uk (S. Galloway).

https://doi.org/10.1016/j.esr.2022.100974
Received 30 May 2022; Received in revised form 11 August 2022; Accepted 7 October 2022
Available online 12 October 2022

Nomenclature

Sets

$\boldsymbol{B}_{mg}$	Set of Low Voltage (LV) branches in a minigrid, *mg*
$\boldsymbol{B}_{mv}$	Set of Medium Voltage (MV) branches, $\boldsymbol{B}_{mv} \in \boldsymbol{B}$
$\boldsymbol{N}_{mg}$	Set of nodes within a minigrid network, $\boldsymbol{N}_{mg} \in \boldsymbol{N}$
$\boldsymbol{\psi}_{mg}$	Set of minigrid branches whose power flow is affected by output of the local generation
$\boldsymbol{B}$	Set of all branches in the networks
$\boldsymbol{G}$	Set of generators connected to the minigrid networks
$\boldsymbol{MG}$	Set of minigrid networks
$\boldsymbol{N}$	Set of nodes in the networks
$\boldsymbol{TFR}$	Set of transformers connecting the MV and minigrid networks

Indices

mg	Index for an individual minigrid
km or *mn*	Indices for network branches
k, m, n	Indices for network nodes
h	Index for hour of the day
z_{mg}	Index of point of grid infeed into a minigrid, *mg*

Parameters

C_{energy}	Cost of energy [c$/kWh]
C_{mv}	Cost of MV network expansion [$/km]
$C_{tfr,S}$	Cost of MV/LV transformer of capacity *S* kVA [$]
L_{mn}	Length of network branch *mn* [km]
R_{mn}	Resistance of network branch *mn* [Ω]
X_{mn}	Reactance of network branch *mn* [Ω]
d	Discount rate [%]
y	Project life span [years]

Variables

C_{inv}	Total annual investment cost [$]
C_{loss}	Total cost of losses [$]
CRF	Investment cost recovery factor
I_{mn}	Current through network branch *mn*
P_g^{mg}	Active power generated by generator *g* of minigrid *mg*
$P_{loss,h}^{mg,z_{mg}}$	Hourly power loss within a minigrid with node z_{mg} as point of grid infeed
$P_{loss,h}^{mv}$	Power loss in the medium voltage network at a certain hour of the day
P_m^D	Active power demand at any network node *m*
P_m^S	Active power supply at any network node *m*
P_{mn}	Active power through network branch *mn*
Q_g^{mg}	Reactive power generated by generator *g* of minigrid *mg*
Q_m^D	Reactive power demand at any network node *m*
Q_m^S	Reactive power supply at any network node *m*
Q_{mn}	Reactive power through network branch *mn*
$\sigma_{z_{mg}}^{mg}$	Binary value for the connection between a minigrid and MV network
σ_{mn}	Binary value whether there is a medium voltage branch between nodes *m* and *n*

imperatives using fit-for-purpose and context-specific methods, will become significant beyond achieving electricity access in developing countries [8].

1.1. Beyond electricity access

Beyond meeting electricity access goals in SSA, the grid is expected to continue expanding and eventually converge and integrate with "grid-akin" offgrid systems like minigrids [11,12]. In Refs. [13,14], authors report this convergence in Southeast Asia, where some minigrids were integrated with the main grid and some were abandoned. With about half a billion people, mostly from developing countries, earmarked to gain initial access to electricity through minigrids by 2030 [15], issues surrounding the future grid integration of minigrids should not be an afterthought to ensure their usefulness beyond grid arrival. The possibility of future grid convergence and integration of minigrids introduces various policy, regulatory and business challenges, some of which are highlighted and significantly addressed in Refs. [13,16,17]. Some of the commercial challenges are addressed in the in-country minigrid regulatory frameworks, for example [18], that define things like conditions for allowing grid integration of minigrids, determination of compensations to minigrid owners and operators, minimization of stranded asserts, and post-grid-integration business models. When a decision is made to integrate a minigrid to an incoming grid, for example using guidelines in Ref. [15], the actual integration introduces technical challenges that need addressing and potential opportunities such as loss reduction and voltage profile improvement, to be exploited [4].

Authors in Ref. [19] suggest that the main technical challenge in the grid integration of formerly offgrid minigrids is the compatibility of technologies (e.g. operating voltage), control and protection philosophies of the two systems. To address voltage incompatibilities during future grid integration, current policies propose that minigrids are designed to operate at the same voltage level as the national grid's secondary distribution lines [18,20]. Alternatively, various power electronics solutions have been proposed to interface with incompatible voltage levels, such as an energy router [19] and a back-to-back converter [21]. Similarly, outputs from the growing literature on network resilience and islanding have also provided several solutions that can be adopted to address control and protection challenges [22,23].

According to Ref. [4], network loss reduction and voltage profile improvement are two main opportunities in the grid integration of minigrids. This argument assumes that minigrid distributed energy resources (DERs) will have the same loss reduction and voltage profile improvement impact as reported for DERs deployed in mature networks in the global north, such as [24]. However, the argument in Ref. [4] does not indicate how such benefits can be accrued, considering the contextual differences between DER deployment in the global north and grid integration of minigrids in the global south. Notably, the positive impacts of DERs in the global north are associated with their optimal placement, sizing, and selection [24] during installation into an existing matured network. On the contrary, during the grid integration of minigrids in SSA, the grid shall integrate with minigrids having an existing network whose DERs were initially placed, sized, and selected to primarily meet offgrid demand, not reduce losses or improve voltage profile.

Since minigrid DERs are deployed prior to grid arrival and without considering loss reduction and voltage improvement objectives, their size, location, and selection cannot be variables for optimal grid integration unless de-rating or re-location are considered as options. Authors in Refs. [25,26] argue that the optimal identification of the point of grid infeed into existing minigrids can lead to better post-integration performance. Nevertheless, the work presented in Refs. [25,26] has three main limitations. Firstly, the authors do not offer a comprehensive formulation for investigating the specified problem. Secondly, the work does not consider the investment cost required to extend the grid from its initial point of termination to the desired optimal grid infeed point in a minigrid. Thirdly, both papers only consider a single minigrid network and do not provide any approach to how optimality can be achieved

when the grid integrates with a cluster of previously autonomous minigrids.

1.2. Article contribution and organization

The aim of this paper is to propose, formulate and test a methodology that is fit for addressing a unique challenge of planning the grid integration of formerly autonomous minigrids in developing countries beyond achieving universal energy access. The paper's first objective is to establish the need and the lack of appropriate methodology for planning the grid integration of minigrids. The second is to apply formal distribution network planning techniques to obtain a mathematical formulation of the proposed method and thirdly, to test the proposed methodology on the grid integration of minigrid networks akin to those in developing countries.

The paper advances the work reported in Refs. [25,26] by presenting a novel minigrid integration planning (MGIP) methodology for systematically planning the grid integration of formerly autonomous minigrids (whether single minigrid or a cluster of minigrids). It takes a distribution network planning approach for quantifying and optimizing the benefits of grid integration of minigrids which is novel considering that such an approach is not considered in any of the prior publications on the grid integration of minigrids in developing countries, such as [4, 13,14,17,19,27]. As an advancement to work reported in Ref. [24], this paper presents a comprehensive formulation adaptable to planning the grid integration of any number of minigrids. The effectiveness of the proposed methodology is demonstrated by comparing its outcomes to those of grid integration planning of minigrids using the empirical approach proposed in Ref. [19], where the authors suggest that the point of grid infeed should be as close as possible to the existing minigrid generator. Unlike in Ref. [19], this paper presents a systematic approach to identifying such points of grid infeed which, in many cases, are away from the minigrid generation hub.

The remainder of the paper is organized as follows. Section II presents the formulation of the problem under investigation, and the optimization approach employed to solve the problem is in Section III. Section IV presents a case study involving integrating the main grid with a single minigrid and a cluster of twelve minigrids mimicking a post-SDG7 scenario in SSA. The case study results are presented and discussed in Section V, and Section VI concludes the paper.

2. MGIP problem formulation

The formulation of MGIP includes the mathematical formalization of the minigrid integration planning problem. However, before the MGIP objective and constraints are presented, key MGIP variables are highlighted and discussed first.

2.1. Key MGIP variables

To highlight the critical MGIP variables, consider a medium voltage (MV) network of the main grid approaching a cluster of minigrids, operating at low voltage (LV), requiring grid integration by extending the grid to each minigrid in a radial topology from the man grid's terminal point, z_{grid}, as shown in Fig. 1. In that case, the key variables will be the grid infeed points, transformer sizes for integrating the incoming MV network and existing minigrid networks and the length of the MV network between the grid terminal point z_{grid} and the grid infeed points for each minigrid.

For each of the network branches within the minigrids or the expanding MV network, the notation illustrated in Fig. 2 applies. In this notation, $S_{km,t}$ and $S_{mn,t}$ are the complex power flowing through any branch of the network at any point in time while Z_{km} and Z_{mn} are the complex impedances of those branches. Then $S^{d}_{m,t}$ is the complex demand at any node m of the network, $S^{g}_{m,t}$ is the complex power generated at node m, and $S^{st}_{m,t}$ is the complex power from or into the storage device at node m whose real part is negative when charging and positive when discharging.

2.2. MGIP objective function

Adopting a static Distribution Network Problem (DNP) [28]

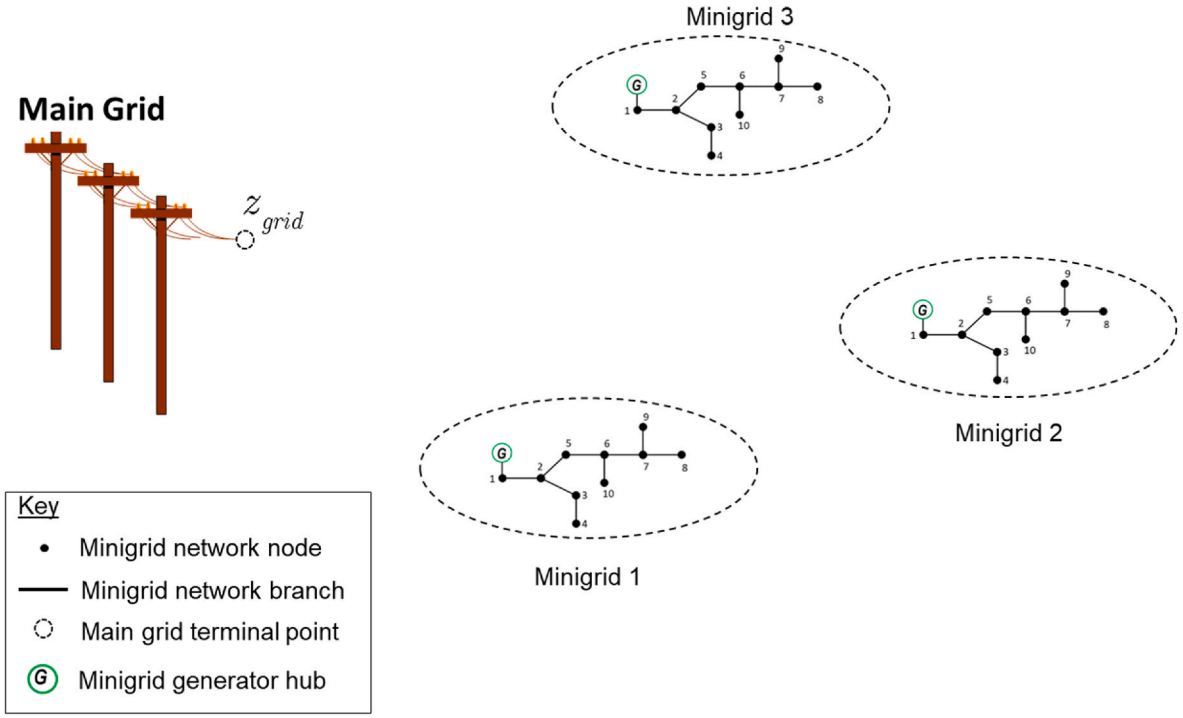

Fig. 1. Arrival of the main grid to a to a cluster of representative three minigrids. Minigrids 1 to 3 assume identical networks for illustrative purposes. It is less likely that a cluster of minigrids will have identical networks. However, the proposed formulation applies regardless of the similarity of the concerned minigrid networks.

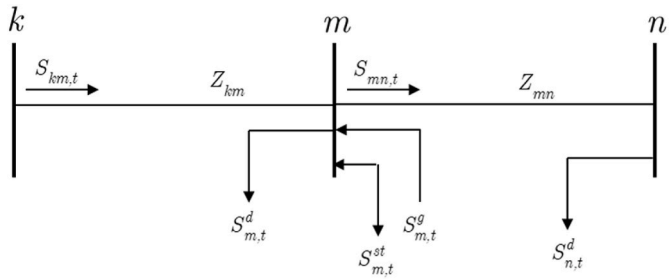

Fig. 2. Network branch notation for MGIP problem formulation.

formulation, the objective function for the grid integration of a cluster of autonomous minigrids is:

$$\min \mathbf{f} = C^{inv}_{ann} + C^{loss}_{ann} \tag{1}$$

Where C_{inv} is the annualized investment cost of the integration, and C^{loss}_{ann} is the annual cost of losses in the integrated network. Prior evidence from distribution network optimization suggests that losses are directly correlated with voltage profile improvement [29]. Hence, the voltage profile has not been explicitly modelled (1), but is later illustrated in the results section.

The annual investment costs, C^{inv}_{ann}, accounts for MV network expansion to each of the minigrid networks in the cluster, and the cost of MV/LV transformer, located at a specific point, z_{mg}, for each minigrid, *mg*. This formulation assumes grid compatible minigrids, a feature in recent minigrid regulation frameworks [16], which do not require any reinforcements during integration with the main grid. The annual investment costs are given by (2):

$$C^{inv}_{ann} = CRF\left(C_{mv}\sum_{mn\in \boldsymbol{B}_{mv}} \sigma_{mn} L_{mn} + \sum_{\substack{mg\in \boldsymbol{MG} \\ z_{mg}\in \boldsymbol{N}_{mg} \\ tfr\in \boldsymbol{TFR}}} C^{tfr}_{z_{mg}}\right) \tag{2}$$

Where *CRF* is the annual cost recovery factor , σ_{mn} is a binary value indicating the presence or absence of an MV network branch *mn*, C_{mv} is the cost of MV network per unit length, L_{mn} is the length for a network branch *mn*. $C^{tfr}_{z_{mg}}$ is the cost of a transformer connecting the main grid and minigrid *mg* at grid infeed point z_{mg}.

The CRF is defined as follows [30]:

$$CRF = \frac{1}{\left(\frac{1}{d} - \frac{1}{(1+d)^{y}}\right)} \tag{3}$$

where *d* is the discount rate per annum, and *y* is the evaluation period in years.

The annualized cost of losses is obtained as follows:

$$C^{loss}_{ann} = 365 \times C_{energy}\sum_{h=1}^{24}\left(P^{mv}_{loss,h} + \sum_{mg\in \boldsymbol{MG}} P^{mg,z_{mg}}_{loss,h}\right) \tag{4}$$

where C_{energy} is the cost of energy per kWh, $P^{mv}_{loss,h}$ is the hourly power loss in the MV network and $P^{mg,\,z_{mg}}_{loss,h}$ is the hourly power loss within minigrid *mg* when the transformer connecting that minigrid to the MV network is placed at a node z_{mg}. The hourly power loss for the MV grid, $P^{mv}_{loss,h}$, is given by,

$$P^{mv}_{loss,h} = \sum_{mn\in \boldsymbol{B}_{mv}} \frac{R_{mn}}{V^2_{n,h}}\left(P^2_{mn,h} + Q^2_{mn,h}\right) \tag{5}$$

Where $\boldsymbol{B}_{mv}$ is a set of all network branches in the MV network and *mn* represents a single network branch with resistance R_{mn} ohms, and receiving end voltage of $V_{n,h}$. The active and reactive power through any minigrid branch, *mn*, at any hour *h*, is given by $P_{mn,h}$ and $Q_{mn,h}$ respectively.

The power loss within any of the minigrids of the cluster, $P^{mg,\,z_{mg}}_{loss,h}$, is given by (6).

$$P^{mg,z_{mg}}_{loss,h} = \sum_{mn\notin \boldsymbol{\psi}_{mg}} \frac{R_{mn}}{V^2_{n}}\left(P^2_{mn,h} + Q^2_{mn,h}\right) + \sum_{mn\in \boldsymbol{\psi}_{mg}} \frac{R_{mn}}{V^2_{n}}\left(\left(P_{mn,h} - P^{g}_{n,h} - P^{st}_{n,h}\right)^2 + \left(Q_{mn,h} - Q^{g}_{n,h} - Q^{st}_{n,h}\right)^2\right), \forall (mn)\in \boldsymbol{B}_{mg}, \forall m,n \in \boldsymbol{N}_{mg} \tag{6}$$

Here, $\boldsymbol{\psi}_{mg}$ is a set of minigrid branches whose active and reactive power flows are affected by the excess power flow from the minigrid generator or storage. For example, if Minigrid 1 in Fig. 1 was connected to the grid through Node 4, the membership of $\boldsymbol{\psi}_{mg}$ will be $\boldsymbol{\psi}_{mg} = \{l_{12}, l_{23}, l_{34}\}$. Also, $P^{g}_{n,h}$ and $Q^{g}_{n,h}$ are the active and reactive power quantities generated by the minigrid generator at any time h, and $P^{st}_{n,h}$ and $Q^{st}_{n,h}$ are the hourly active and reactive power quantities from/into the storage within the minigrid. The rest of the terms are as defined previously. Besides affecting the power losses within the minigrid, the points of grid infeed into the minigrids also affect the length of the MV network required to integrate the minigrids to the main grid.

The objective function formulation presented in (1) – (5) assumes that the MV network does not host any distributed energy resources; hence (5) is a passive branch-flow-model loss equation. However, (6) recognizes the impact of the point of grid infeed (or transformer location) on the power flows in the minigrid network as any selection of the grid infeed point, z_{mg}, splits the minigrid network branches into two sets. Firstly, a set of network branches whose power flow, compared to the power flow when the point z_{mg} and the DG are co-located, is affected by the output of the local (or residual) generator, $\boldsymbol{\psi}_{mg}$. Secondly, a set including branches whose power flow is not affected by the generators' production.

2.3. MGIP constraints

The MGIP objective function in (3) is subject to the following equality and inequality constraints for every hourly evaluation.

2.3.1. Power flow constraints

The first set of equality constraints for the evaluation of MGIP will come from power flow equations. Recalling Fig. 2, the active and reactive power balance at each network node, say *m*, will be respectively given by (7) and (8).

$$\sum_{km\in \boldsymbol{B}} P_{km,h} - \sum_{mn\in \boldsymbol{B}}\left(P_{mn,h} + R_{mn} I^2_{mn,h}\right) + P^{g}_{m,h} + P^{st}_{m,h} - P^{d}_{m,h} = 0; \forall k,m,n \in \boldsymbol{N} \tag{7}$$

$$\sum_{km\in \boldsymbol{B}} Q_{km,h} - \sum_{mn\in \boldsymbol{B}} \left(Q_{mn,h} + X_{mn} I^2_{mn,h}\right) + Q^g_{m,h} + Q^{st}_{m,h} - Q^d_{m,h} = 0; \forall k, m, n \in \boldsymbol{N} \tag{8}$$

where (7) ensures that there is an active power balance on all network nodes, i.e., the incoming active power at any node is equal to the outgoing. Similarly, (8) ensures a reactive power balance on all nodes in the network.

The voltage drop across any network branch is given by (9)

$$V^2_{m,h} - V^2_{n,h} = 2\left(R_{mn} P_{mn,h} + X_{mn} Q_{mn,h}\right) + \left(R^2_{mn} + X^2_{mn}\right) I^2_{mn,h}; \forall (mn) \in \boldsymbol{B}, \forall m, n \in \boldsymbol{N} \tag{9}$$

and the square of the current, appearing in (7) to (9), through each network branch is given by (10)

$$I^2_{mn,h} = \frac{P^2_{mn,h} + Q^2_{mn,h}}{V^2_{n,h}}; \forall (mn) \in \boldsymbol{B}, \forall m, n \in \boldsymbol{N} \tag{10}$$

The power flow constraints for MGIP, presented in (7) to (10), show that MGIP is a non-linear model as they contain a mixture of multiplication and squaring of terms at various points.

2.3.2. Voltage limits

The first inequality constraint for this problem will be that the voltages at all network nodes are within a set band, as follows in (11). In this paper, the voltage is set to be within ±0.1 pu of the nominal voltage [31].

$$V_{min} \le V_{m,h} \le V_{max} \forall (m) \in \boldsymbol{N} \tag{11}$$

2.3.3. Thermal and capacity limits

Another set of inequality constraints comes from the network assets' thermal and capacity ratings as follows:

$$0 \le P^g_{m,h} \le P^{g,max}_m; \forall g \in \boldsymbol{G}, \forall m \in \boldsymbol{N_{mg}} \tag{12}$$

$$S^{min}_{tfr} \le S^{mg}_{tfr,h} \le S^{max}_{tfr}; \forall tfr \in \boldsymbol{TFR}, \forall mg \in \boldsymbol{MG} \tag{13}$$

$$\left|I_{mn,h}\right| \le I^{max}_{mn}; \forall (mn) \in \boldsymbol{B} \tag{14}$$

$$0 \le \left|P^{st}_{m,h}\right| \le P^{st,max}_m; \forall st \in \boldsymbol{ST}, \forall m \in \boldsymbol{N_{mg}} \tag{15}$$

$$C^{st,min}_m \le C^{st}_{m,h} \le C^{st,max}_m; \forall st \in \boldsymbol{ST}, \forall m \in \boldsymbol{N_{mg}} \tag{16}$$

where (12) ensure that the thermal limits of generators are observed, (13) is for transformer capacity limits, (14) is for the thermal limits of the network lines, and (15) and (16) are constraints for storage devices within the minigrid networks.

3. MGIP problem evaluation

The problem defined in (1) - (16) is characterized as a mixed-integer non-linear problem (MINLP) with three integer (or discrete) variables, namely, the points of grid infeed, size of transformer and MV network layout. The non-linearities in this problem originate from squaring and multiplication of terms in (7) to (10). Both classical and modern optimization techniques have been successfully applied to solve similar problems as reported in Ref. [29]. Due to the lack of established, off-the-shelf MINLP solvers, using classical techniques involves linearising and approximating the problem to obtain an equivalent Mixed-Integer Linear Program (MILP) [32,33]. This approach is preferred because of its scalability and guarantee of global optimality for the reduced problem. However, it can lead to an infeasible solution as linearisation and approximation alter the original problem's characteristics. For this reason, the MGIP problem presented in this paper is solved using a modern optimization technique of Genetic Algorithm (GA), which has also been applied in similar planning problems such as [34]. The implementation of this methodology is as summarised in Fig. 3.

In Fig. 3, the MGIP methodology accepts inputs such as minigrid network models with geo-referenced (or cartesian referenced) nodes to identify points of grid infeed into the minigrids, calculate MV network lengths, and reticulation. The MV network terminal location, minigrid loads and load profiles, residual photovoltaic (PV) generation capacities in the minigrids, candidate MV/LV transformers and their costs, MV network costs, and investment parameters such as discount rates and evaluation period are required.

Once all the input parameters are supplied, the GA randomly generates an initial population of feasible chromosomes for any j number of minigrids in the cluster, which satisfy (7) to (16). A minimum spanning tree connecting the MV network to all minigrids in the cluster is obtained for each feasible chromosome. Then, the fitness function (1) is evaluated, and the first-generation parent is selected.

After that, GA operators of cross-over, mutation and elitism selection are used to obtain a new parent for the subsequent generations until a termination criterion is met. The GA applied in this methodology terminates when the change in the fitness function is below 10^{-6} or the number of generations exceeds $200 \times j$.

4. MGIP case studies

The MGIP method presented in this paper is applied to two grid integration planning of minigrids case studies. The first case study investigates the grid integration of a single minigrid by exploring several combinations of minigrid demand and DERs to highlight the main drivers of the MGIP solution. The second case study involves the grid integration planning of a cluster of twelve minigrids, demonstrating the application of MGIP to a more extensive planning problem.

Fig. 4 shows the main grid point A, a single minigrid, and a cluster of twelve (12) minigrid networks (adapted from Ref. [35]) used in the case studies reported in this paper. The nodes in each network are numbered sequentially, similar to the illustrative example in Fig. 1. There are two main reasons that support the suitability of applying these networks to the assess the MGIP problem.

Firstly, the IEEE Test Feeder Working Group[1] recommends that any test feeder can be used to investigate microgrid (or minigrid) related problems [36]. A survey of the available test networks [37] reveals that the network in Fig. 4(a), is one of the low capacity and low voltage IEEE test networks comparable to minigrids in SSA. Since the network in Fig. 4(a) is originally from Ref. [35], the rest of the networks from Ref. [35] are considered useful. Secondly, the networks represent a trunk-and-branch topology that mimics minigrids in developing countries [10]. The cluster of minigrids in Fig. 4(b) was created by randomly placing the available test networks at different distances and orientations from the terminal point without any perceived 'favourable' allocation or order. The presented example is one of several studies conducted on this cluster of minigrids and in each case, the location and orientation of the minigrid networks were changed.

Table 1 summarises the details of the minigrid networks in Fig. 4(b). The details of the network in Fig. 4(a) are the same as for minigrid #1 in Table 1.

Different combinations of demand and residual DER profiles presented in Fig. 5 are applied in the minigrids of this case study. Fig. 5 (a)–(c) illustrates low (LW), medium (MD) and high (HG) load factor demand profiles to account for different demand conditions. Fig. 5 (a) is based on those provided in Ref. [38], this is a demand profile with a low demand factor of 21%. It is a baseline demand factor for minigrids without any forms of economic use of energy or electric cooking, similar

[1] https://cmte.ieee.org/pes-testfeeders/.

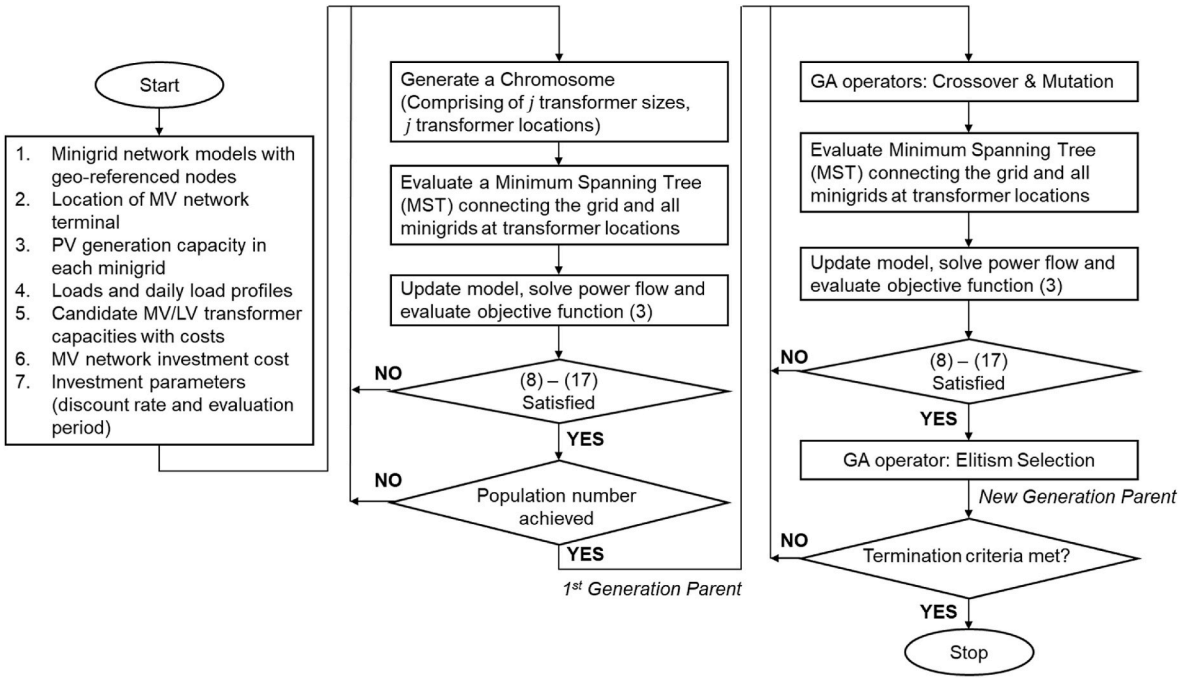

Fig. 3. Flowchart of the Genetic Algorithm implementation of the MGIP methodology.

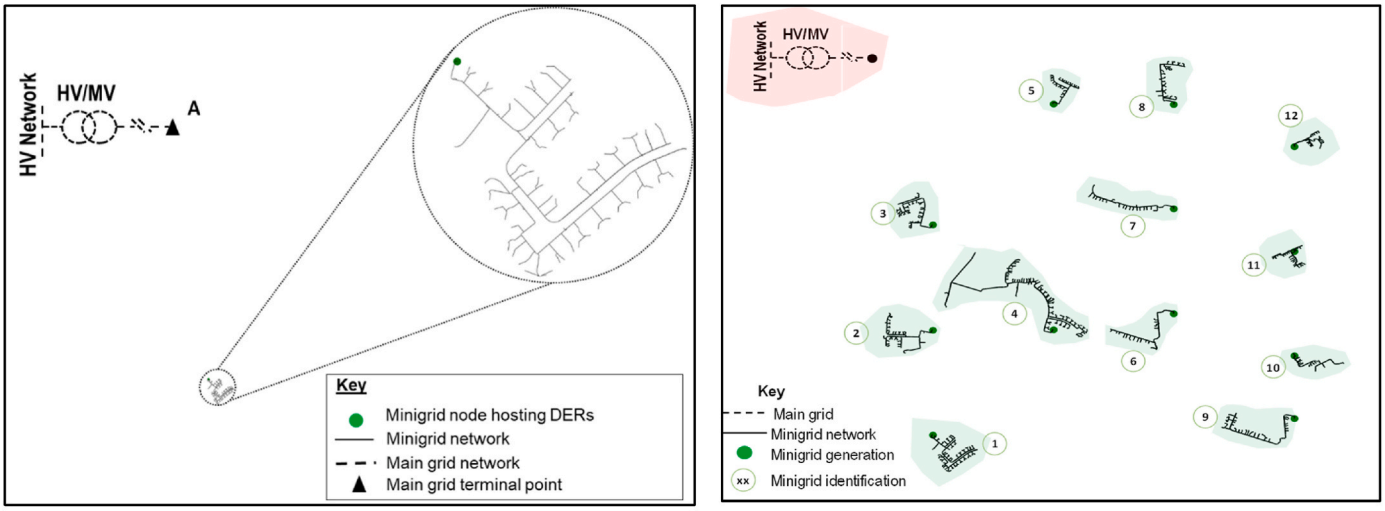

(a) Single minigrid for grid integration *(b) A cluster of minigrids for grid integration*

Fig. 4. The main grid approaching a cluster of twelve minigrids.

Table 1
Key details of the case study (adapted from Refs. [35,37]).

Minigrid Property	Minigrid ID											
	#1	#2	#3	#4	#5	#6	#7	#8	#9	#10	#11	#12
Peak Demand (kW)	250	80	160	200	80	60	75	90	100	40	55	35
Number of Nodes	205	111	123	341	58	232	97	61	144	194	240	134

to the work reported in Ref. [15]. Fig. 5 (b) is adapted from the profiles in Ref. [38] to obtain a mid-range load factor of 46% which is between the baseline minigrid demand factor of 22% and the highest demand factor of 80% described in Ref. [15]. Fig. 5 (c) is based on data from Ref. [39], this demand profile has a high demand factor of 69%. Although this is lower than the high demand factor of 80% suggested in Ref. [15], it represents a realistic value as grid level demand factors can reach around 70% [40].

The profiles in Fig. 5 (d)–(f) account for individual or combination residual DERs in minigrids in developing countries. Fig. 5 (d) is representative of an ideal daily photovoltaic generation profile for a SSA region based on data from Ref. [41]. Fig. 5 (e) is a profile that assumes that

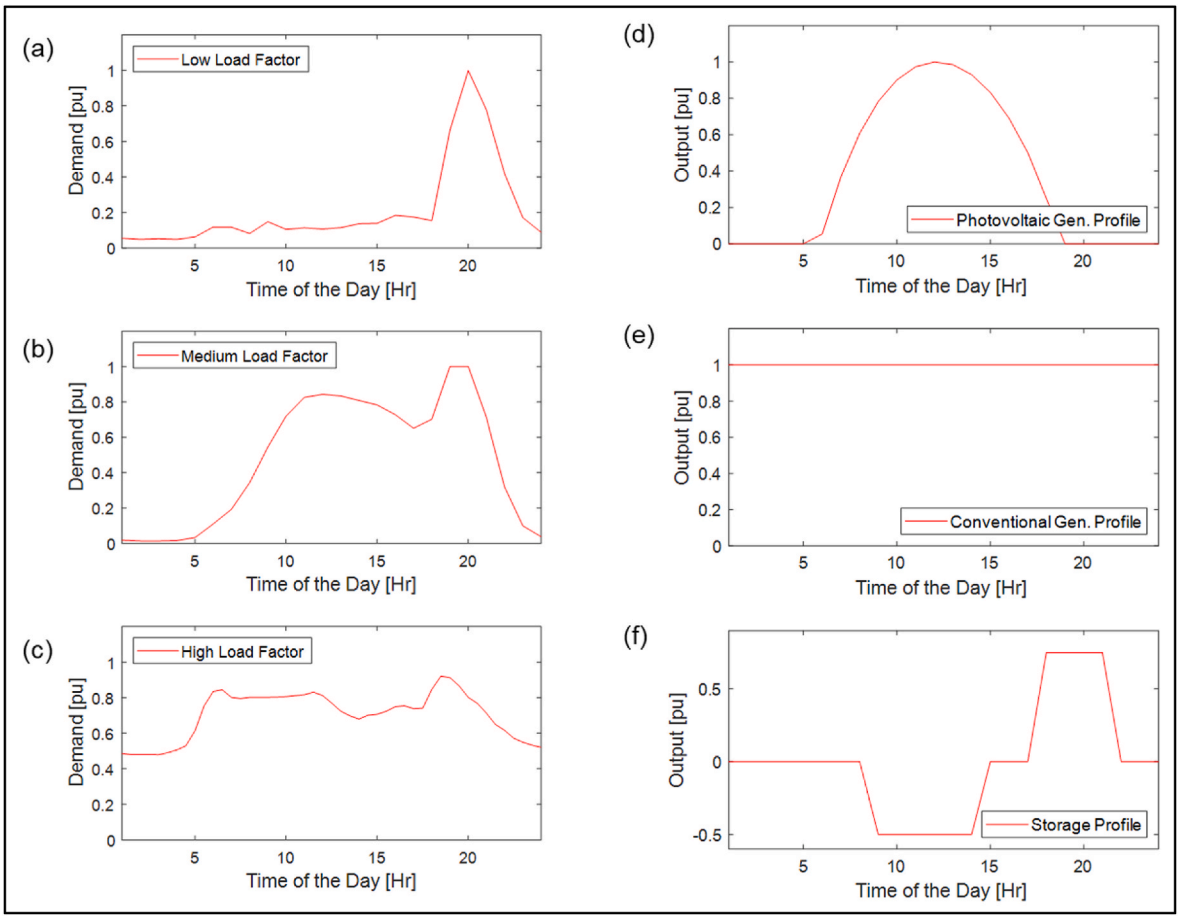

Fig. 5. Generator, storage, and demand profiles for MGIP case studies [10,15,38,41,42].

Table 2
MGIP case study scenarios.

Case study ID	Minigrid network	Minigrid DER	Demand Profile
Case study 1	Single minigrid	PV, PV + Storage, Conventional generator	LW, MD, HG*
Case study 2	Cluster of minigrids	PV	MD

*LW = Low load factor. MD = Medium load factor. HG = High load factor.

a conventional generator, for example a mini hydro power plant, is generating at full power output for 24 h of the day. Fig. 5 (f) shows a profile for charging and discharging the minigrid storage. The storage is charged during the day when PV generation is the highest and discharged in the evening when demand is high. It an adapted combination of peak shaving in Ref. [42] and cycle-charging in Ref. [10].

In both case studies, a conservative project period of 15 years and a discount factor of 10% are used [10,43]. The cost of MV line, MV/LV transformers and cost of energy (12c$/kWh) are also derived from Refs. [10,43].

Table 2 presents a summary of the two case studies reported here. Case study ID identifies the case study, minigrid network states which network (from Fig. 4) is used, minigrid DER specifies the residual DER in the minigrid networks, and the demand profile sets the level of demand in the minigrid. In each of the case studies in Table 2, the penetration of DERs is varied from 0 to 100%.

The proposed MGIP method is compared to ***No-Opt,*** where the grid infeed points for each minigrid collocate with the residual DERs in that minigrid. This is based on the recommendation in Ref. [19], where the authors suggest that during grid integration of formerly autonomous minigrids, the grid incomer should be connected as close to the minigrid DER as possible. The transformer capacities in No-opt are decided by choosing the transformer size with a higher thermal capacity than the known peak power demand in the minigrid.

Table 3
MGIP grid infeed points for grid integration planning of single minigrid with various DERs and demand profiles.

DER Type		PV			PV + Storage			Conv. generator		
Demand profile		*LW*	*MD*	*HG*	*LW*	*MD*	*HG*	*LW*	*MD*	*HG*
DER Penetration.*	*0%*	46	46	46	46	46	46	46	46	46
	20%	46			46			39	46	46
	40%	20			43			1	46	94
	60%	5			37			1	20	46
	80%	1			1			1	1	1
	100%	1			1			1	1	1

DER Penetration – DER peak power capacity as a percentage of minigrid peak demand [47].

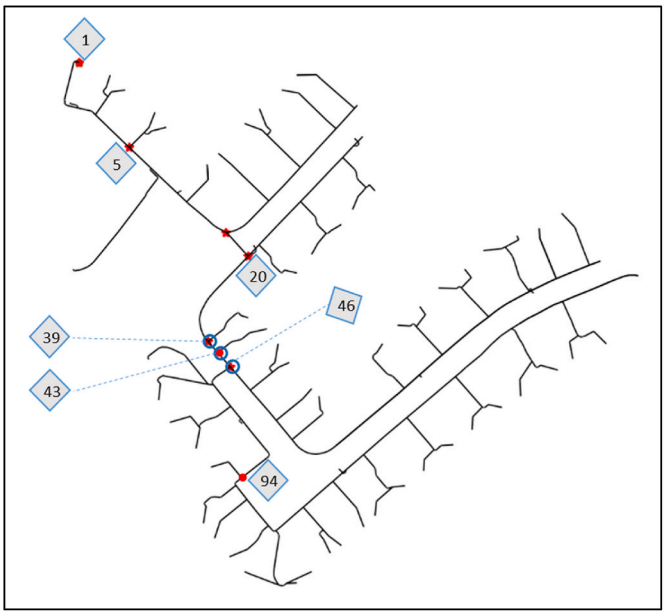

Fig. 6. Location of grid infeed points reported in Table 3.

5. Results and discussion

The results of applying the MGIP method to the case study scenarios defined above are presented and discussed as follows:

5.1. Case study 1 – MGIP on a single minigrid

5.1.1. Grid infeed points and transformer sizes

Table 3 shows the optimal grid infeed points realized from using MGIP in planning the grid integration of a single minigrid under different loading and DER conditions. The locations of the identified points of grid infeed are shown in Fig. 6. For comparison with No-opt, the grid infeed point for all DER and load scenarios is Node 1, where the minigrid generation hub is located as recommended in Ref. [19].

Table 3 and Fig. 6 show that MGIP identifies Node 46 as a popular grid infeed point for different DER and demand combinations. For example, Node 46 is the only optimal grid infeed point for all PV and PV + storage penetration scenarios under medium and high demand factors. Although there is a mixture of different points of grid infeed for the other combinations of DERs and load profiles, Node 46 is still one of the solutions. When compared with the No-opt grid infeed solution (Node 1), it is observed that the MGIP characteristic grid infeed node is not the node that hosts the minigrid DERs, Node 1 in this case. These results show that MGIP can identify a characteristic grid infeed point for a minigrid. For minigrids with a trunk and branch topology [10,44], as investigated in this case study, the characteristic grid infeed point is less likely to be at the node that hosts the minigrid generator or DERs.

Besides identifying a characteristic node of grid infeed for the minigrid, Table 3 and Fig. 6 also show that increasing DER penetration moves the MGIP generated optimal grid infeed point away from the characteristic node and close to the node hosting the residual DER. In Table 3, this observation is accurate for low load profile with PV and PV + storage and all load scenarios when a conventional generator is connected. For PV and low load profile, the point of grid infeed is Node 46 at 0% DER penetration. However, this MGIP generated optimal grid infeed node becomes Node 1 from 80% PV penetration. As the DER penetration increases, the positive impacts of having a grid infeed point away from the minigrid generator hub are eclipsed by the adverse effects of the increasing size of the minigrid residual DERs. This point is elaborated further in discussing the objective evaluation results of this case study. Before that, here are the results for transformer sizing for the grid integration of a single minigrid.

Table 4 shows the corresponding transformer sizes for the grid integration of the single minigrid with different demand factors, DERs and DER penetration. For the No-opt method, a comparator to the MGIP, the corresponding No-opt transformer size for all DER types, DER penetration, and load profiles is 315kVA.

Table 4 shows that PV without storage does not affect MGIP transformer sizing as MGIP and No-opt yield the same transformer size, 315kVA for the scenario with residual PV within the minigrid. This should be expected as a PV generator without storage does not influence the evening peak demand into the minigrid [10]. For example, as shown in Fig. 5(d), PV generates an output between 06:00 and 18:00, while the peak demand occurs around 19:00 and 20:00 in the load profiles presented in Fig. 5 (a)–(c). Therefore, as long as the peak demand remains unaltered, which will be the case if a minigrid's only residual DER is PV, the transformer sizes from the power flow based method, MGIP and non-power flow-based, No-opt will remain the same. The only way that PV without storage can influence transformer sizing is when the value of peak power export into the main grid exceeds the value of peak demand in the evening. This scenario would occur for a PV penetration level of considerably higher than 100%. However, the investigation reported in this paper has limited residual PV penetration to 100% of the peak minigrid demand.

While PV generator does not affect the transformer sizing, Table 4 shows that the other DER combinations do. MGIP transformer sizing is affected by PV + Storage and conventional generator. This variety of integration transformer sizes is unlike the results when the PV is used, where only one transformer size of 315kVA was realized. Based on the load factor and DER penetration levels, Table 4 shows that PV + storage and Conventional generator scenarios have 100kVA, 200kVA, and 315kVA as optimal transformer sizes for the integration. For example, in the medium demand factor scenario of PV + Storage, Table 4 shows that 315kVA transformer sizes are optimal for DER penetrations of 0% and 20% while 200kVA transformer sizes for generator penetration of 40%–100%.

The variety in solutions to the transformer sizes can be attributed to energy storage and conventional generation impacting the net power export or import into the minigrid at different times of the day [42]. Since the conventional generator is assumed to be available and generating at full capacity for the entire day, its effect on the peak load is more significant than a PV generator without any storage as it offsets part or all of the minigrid demand throughout the day. Also, since the

Table 4
MGIP transformer sizes (in kVA) for grid integration of a single minigrid with various DERs and demand profiles.

DER Type		PV			PV + Storage			Conv. generator		
Demand profile		*LW*	*MD*	*HG*	*LW*	*MD*	*HG*	*LW*	*MD*	*HG*
DER Penetration	*0%*	315	315	315	315	315	315	315	315	315
	20%				315	315	315	200	200	200
	40%				200	200	200	200	200	200
	60%				200	200	200	200	200	100
	80%				200	200	200	200	200	100
	100%				315	100	200	315	315	200

energy storage discharges some power in the evening hours of the day, it reduces the amount of power required to flow into the minigrid to service the evening peak. The changes caused by storage or conventional generators in maximum net import or export from the minigrid affect the MGIP method's determination of the integration transformer size.

Determining the transformer sizes by observing the magnitude of maximum net power flow between the minigrid and the main grid is vital because it avoids overinvesting in transformers by specifying the smallest transformer size that can accommodate the observed power flow [45]. However, such an approach becomes problematic when the presence of a DER leads to the specification of an integration transformer capacity less than the peak demand and the minigrid DER fails. In such cases, the entire minigrid demand must be supplied from the main grid, and the lower-rated transformer may be a constraint. Given that the peak demand in the minigrid under investigation is 250 kW (see Table 1), a 200kVA or 100kVA integration transformer may not be adequate to serve peak power demand when the incumbent minigrid generator is out of service. Therefore, transformer sizing for minigrid integration should accommodate most of the scenarios in the minigrid network, including incidences of outage on the incumbent minigrid DERs.

Therefore, the results presented in this section demonstrate that, in most cases, the MGIP method identifies grid infeed points that are unique from those of the No-opt method. As the DER penetration capacity increases, the optimal grid infeed points from MGIP move towards the location of the minigrid generator hub (or grid infeed point for the No-opt method). Since one may not intuitively know the tipping point for shifting the best grid infeed point towards the DER hub, the MGIP method systematically identifies a grid infeed point for various demand and DER scenarios. A discussion on the objective evaluation further substantiates the argument above.

5.1.2. *Objective function evaluation for grid integration of a single minigrid*

The annualized costs of integrating the single minigrid, as evaluated from (1), are presented in Fig. 7. The figure comprises the cost of grid

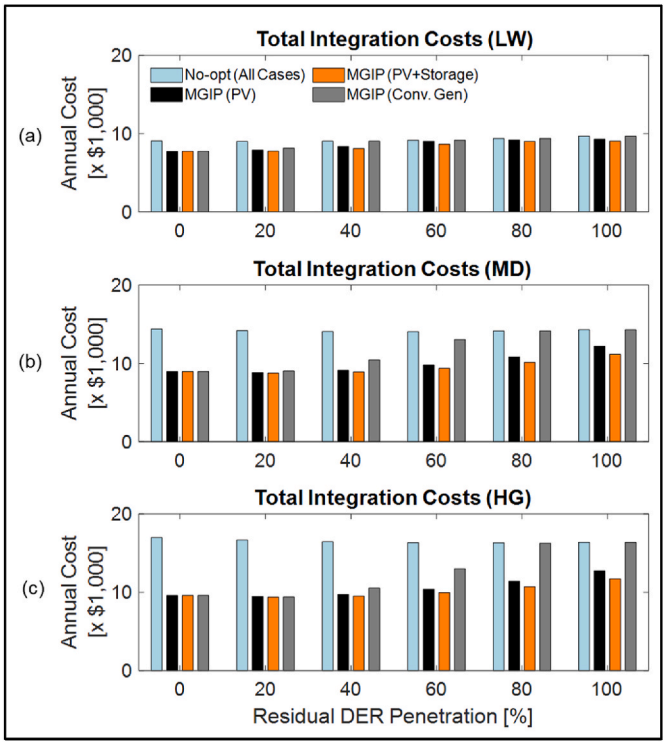

Fig. 7. Annual integration costs for a single minigrid with various DER and demand situations.

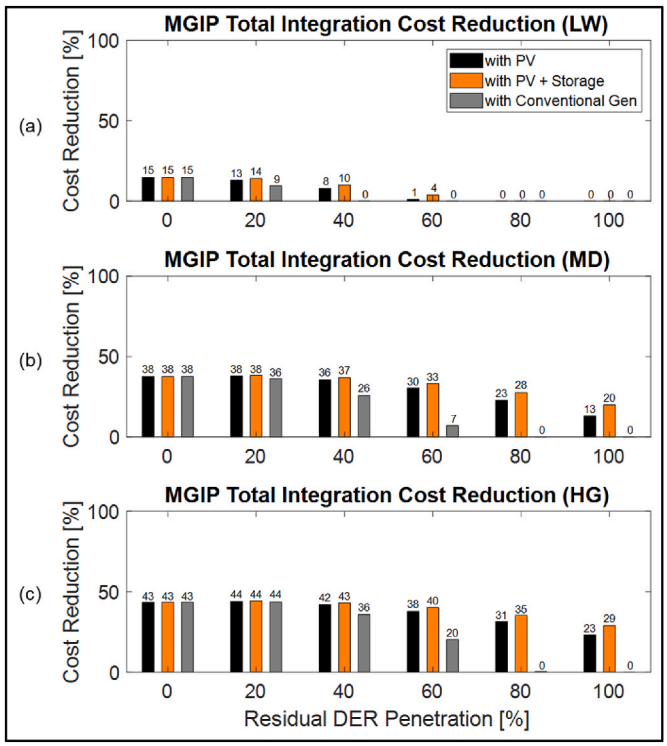

Fig. 8. Cost reduction benefits of MGIP over No-opt.

integration when using MGIP and No-opt for the considered DER and demand scenarios. For each of the considered DER combinations, Fig. 7 (a) reports the integration costs for the minigrid with a low demand factor, while the results in Fig. 7 (b) and (c) are for the minigrid with medium and high demand factors, respectively.

Fig. 8 shows a comparison of No-opt and MGIP costs reported in Fig. 7, highlighting the cost reduction that can be achieved by using MGIP in each of the considered DER and load combinations. Figs. 7 and 8 motivate the following discussion.

A side-by-side comparison of annual integration costs for No-opt and MGIP in Fig. 7 reveals that MGIP leads to lower objective function values in most cases. In the breakdown of the yearly cost of integration, it is evident that the biggest cost differential between MGIP and No-opt comes from the cost of losses component. The key factor driving the post-integration loss performance of the MGIP is the grid infeed point into the minigrid. For example, at 0% DER penetration in Fig. 7, the loss component of the MGIP annual integration cost is significantly less than that of No-opt. The corresponding grid infeed points for all DER scenarios reported in Table 3 are Node 46. Comparing this to the grid infeed point for No-opt, Node 1, it shows that for the same DER and load combinations, the point of grid infeed into the minigrids affects the overall losses and associated cost of the integrated network.

The results in Figs. 7 and 8 show that the economic benefits accrued from the MGIP method increase with an increasing minigrid load factor. For example, Fig. 8 (a)–(c) show that at 0% PV penetration, the annual integration cost of MGIP is 15%, 38% and 43% better than No-opt for low, medium and high demand factors, respectively. This trend can be observed for the other DER scenarios throughout the results in Fig. 8. The benefits of MGIP increase with increasing demand factors because the annual losses significantly influence MGIP benefits. The minigrid has fewer annual losses for low demand factors than medium and high demand factors, as shown in Fig. 7. Therefore, for the same level of loss reduction (as a percentage of initial losses), the annual cost reduction will be higher for a lossy minigrid than for a less lossy one.

Fig. 7 also show that the benefits accrued from the MGIP method generally decrease with an increasing DER penetration compared to the

No-opt method. For example, in the low demand factor scenario in Fig. 8 (a), at 0% PV penetration, the annual integration cost of MGIP is 15% better than No-opt, while at 100% PV penetration, the MGIP is 0% better than No-opt. A similar trend is observed in the other DER situations, PV + storage and conventional generator, in Fig. 8(b) and (c), respectively.

This reduction in MGIP benefits with increasing DER capacity can be attributed to the combined impact of grid infeed point and the size of DERs on the losses within the minigrid network. For higher DER penetration levels, the residual generator in the minigrid does not only serve adjacent demand but also exports some of the excess power to the upstream network through the grid infeed point. When the grid infeed point is away from the minigrid generator location, the higher capacity DER introduces additional power flows in the minigrid. Depending on the size of the minigrid DER, the additional power flow can increase or decrease losses in the minigrid. As the DERs penetration rises further, the extra losses caused by the minigrid generation diminish the loss reduction benefits that were gained through identifying an optimal grid infeed point away from the residual minigrid generator. Consequently, the optimal grid infeed point moves towards minigrid generator hub for higher DER penetration levels, as reported in Table 3.

Fig. 7 shows that the type of residual DER affects the annual cost of minigrid integration. This can be observed in the higher DER penetration levels where the cost of integrating a conventional generator using MGIP is equal to the cost of grid integration using No-opt. However, for higher penetration of PV + storage and PV only, the total MGIP integration cost is still lower than for the No-opt method. A breakdown of the annualized cost in Fig. 7 reveals that the difference in the MGIP benefits for the various DER combinations originates from the cost of losses and not investments. For the modelled case study, the conventional generator leads to a high cost of losses because, upon grid integration, it can generate a constant power output which may be consumed locally or exported from the minigrids. In periods of low demand within the minigrid, the generated power will be largely exported to the upstream grid throughout the day and night. On the other hand, such magnitudes of export cannot be expected for PV or PV + Storage DERs because the PV only generates during the day while a functioning conventional generator, for example hydropower, can generate power both day and night. The effect of DER type can also be noted in Fig. 8 where PV + Storage records the best MGIP cost reduction potential for all the DER penetration levels.

The results presented in this section have demonstrated the superiority of using the MGIP method when integrating a single minigrid into the main grid. For most cases, MGIP recorded a better loss reduction value than No-opt. These results also show that benefits from using MGIP increase with an increasing demand factor in the minigrid and decrease with a rising penetration level of the residual DERs. Also, different combinations of residual DERs have been observed to affect the outcomes of MGIP differently, with PV + storage being the best among the DER combinations investigated here.

Table 5
Points of Grid Connection and Transformer sizes.

Integration Method	PV Pen.	Minigrid ID					
		#1	#2	#3	#4	#5	#6
MGIP	*0%*	46	55	7	151	35	81
	25%	64	75	50	218	6	152
	50%	60	86	31	209	44	156
	75%	60	95	60	207	11	134
	100%	94	67	47	220	18	172
No-Opt	*All*	1	1	1	1	1	1
Integration Method	**PV Pen.**	**Minigrid ID**					
		#7	*#8*	*#9*	*#10*	*#11*	*#12*
MGIP	*0%*	40	42	38	154	73	69
	25%	41	34	102	103	136	29
	50%	53	44	90	156	118	8
	75%	57	25	32	67	71	86
	100%	31	50	6	30	97	72
No-Opt	*All*	1	1	1	1	1	1

5.2. Case study 2 – MGIP on a cluster of minigrids

This case study is presented to demonstrate the flexibility and application of the MGIP in planning the grid integration of a more complex scenario involving more than one minigrid presented in Case study 1. Upon investigating all DER combinations within the cluster, the conclusions were not dissimilar to those drawn from Case study 1 – most of the benefits of using MGIP are drawn from loss reduction. Therefore, for brevity, this section reports the grid integration of a cluster of solar PV minigrids.

5.2.1. Grid infeed points and MV network layout

Table 5 shows the grid infeed points for integrating the respective minigrids to the main grid obtained from both MGIP and No-opt. The node numbers in Table 5 show that MGIP does not result in Node 1 (where the minigrid generators are located) as the optimal point of grid infeed for any of the minigrid networks considered. This is consistent with the previous observation, from Case study 1, that collocating grid infeed with the local generator, as in No-opt, is not optimal from both the MV and minigrid network perspectives.

The differences in grid infeed points identified through No-Opt and MGIP show that the two methods are less likely to lead to a common solution. This difference is further highlighted in the MV network reticulation for the two methods as presented in Fig. 9. Fig. 9(a) shows the MV reticulation for MGIP, specifically, the grid infeed points for PV penetration of 50% in Table 5. Fig. 9(b) shows that MV reticulation for the No-opt method where the grid incomer is collocated with the minigrid generator. The difference in the layout of the MV network in Fig. 9 (a) and (b) illustrate that the points of grid infeed into minigrids also affect the reticulation of the resulting MV network for integrating formerly autonomous clusters of minigrids.

Despite the differences in grid infeed points into the minigrids, both methods lead to the same MV/LV transformer sizes for integrating the main grid with the individual minigrids in the cluster. This is consistent with the PV scenario in Table 4 and the associated discussion also applies here.

5.2.2. Objective function evaluation for grid integration of a cluster of minigrids

Fig. 10 shows the total annualized cost obtained from (1) for the grid integration of the cluster of minigrids, and their breakdown for each of the two methods. Fig. 10(a) shows that No-Opt leads to an overall high annualized cost of integrating the cluster of minigrids compared to the MGIP method in Fig. 10(b). At best, the MGIP case leads to a ~30% reduction in the total annualized cost of the integration than the No-Opt case.

Fig. 10(a) also shows that the No-Opt case's annualized costs reduce with increasing residual PV penetration, while those for MGIP (in Fig. 10 (b)) reduce and then rise again. The breakdown of the cost components shows that, like in the previous case study, the change in annualized cost is significantly influenced by the losses component of the costs and not the investment costs. A detailed discussion on the changes in losses is provided later in this section. Before that, Fig. 11 presents the breakdown of the investment costs, showing the closeness of the investment cost from both methods.

Fig. 11 shows that the annual transformer costs are the same ($4062) for each case, which is expected as it has been previously discussed that both methods yielded the same set of transformer sizes. However, minor differences are observed in the annual line costs as the No-Opt, in Fig. 11 (a), leads to costs of $21,230, but the MGIP results in an average line cost of $23,000. The differences in the annualized investment cost are caused by differences in grid infeed points which affect the MV network reticulation. Since LV minigrid networks will typically cover a small area,

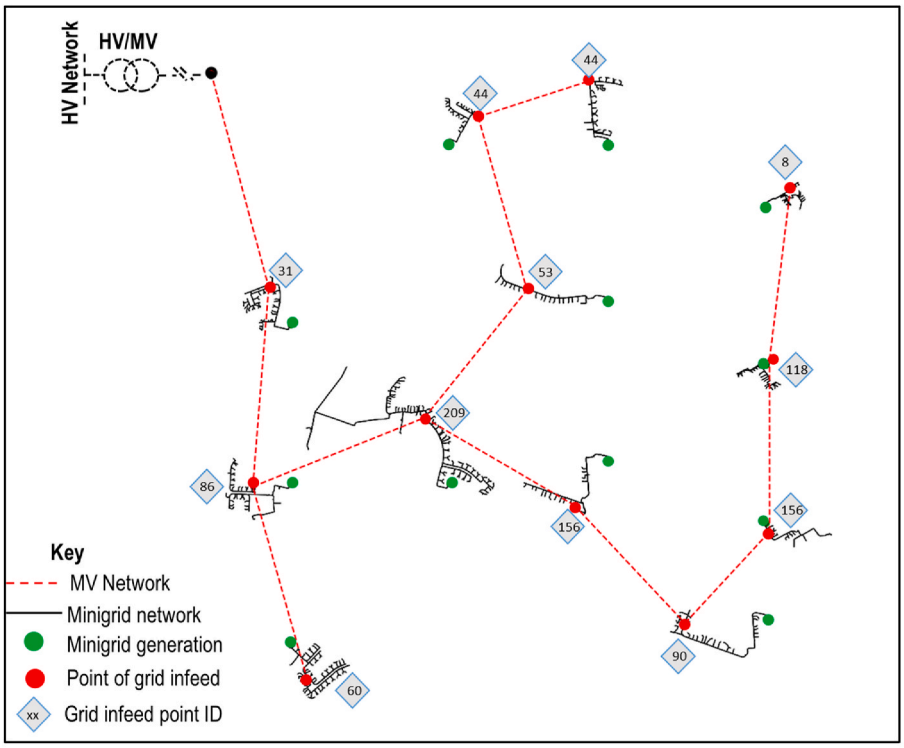

(a) MGIP MV network layout

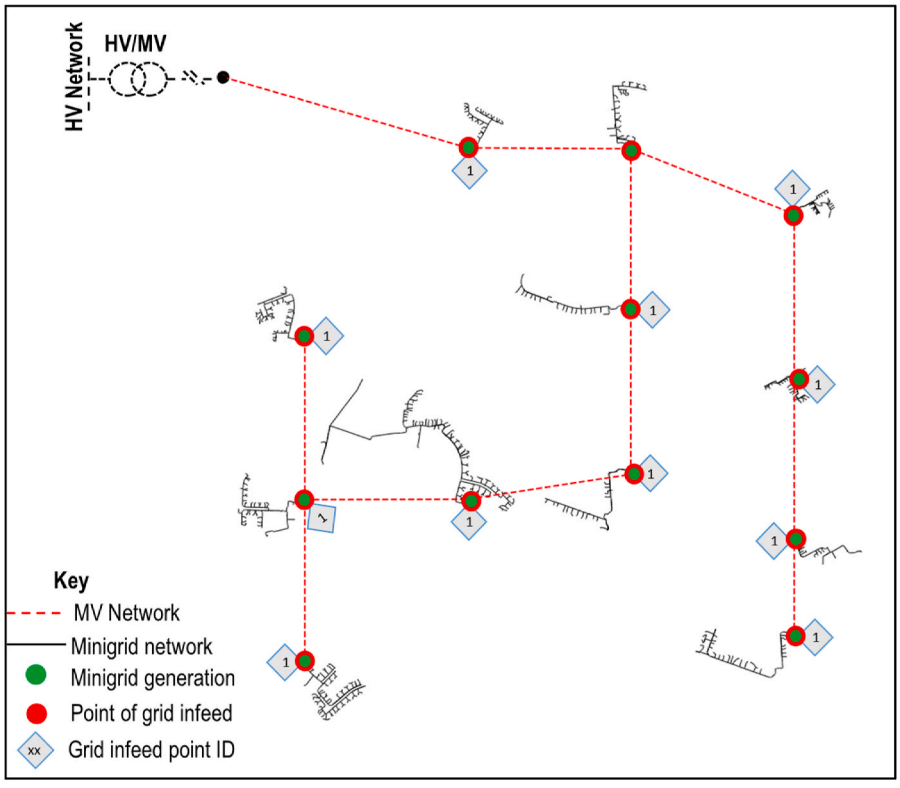

(b) No-opt MV network layout

Fig. 9. MGIP and No-opt MV network reticulation for the grid integration of minigrid cluster.

different grid infeed points will not introduce significant differentials in the total line length. Hence Fig. 11 shows that the investment requirement in No-opt is lower than that of MGIP, but the difference is not very significant.

The results in Fig. 10 demonstrate that the MGIP method yields better annualized cost when losses are included despite a higher investment cost. Therefore, although the investment cost (including the cost of lines and transformers) for the grid integration of clusters of

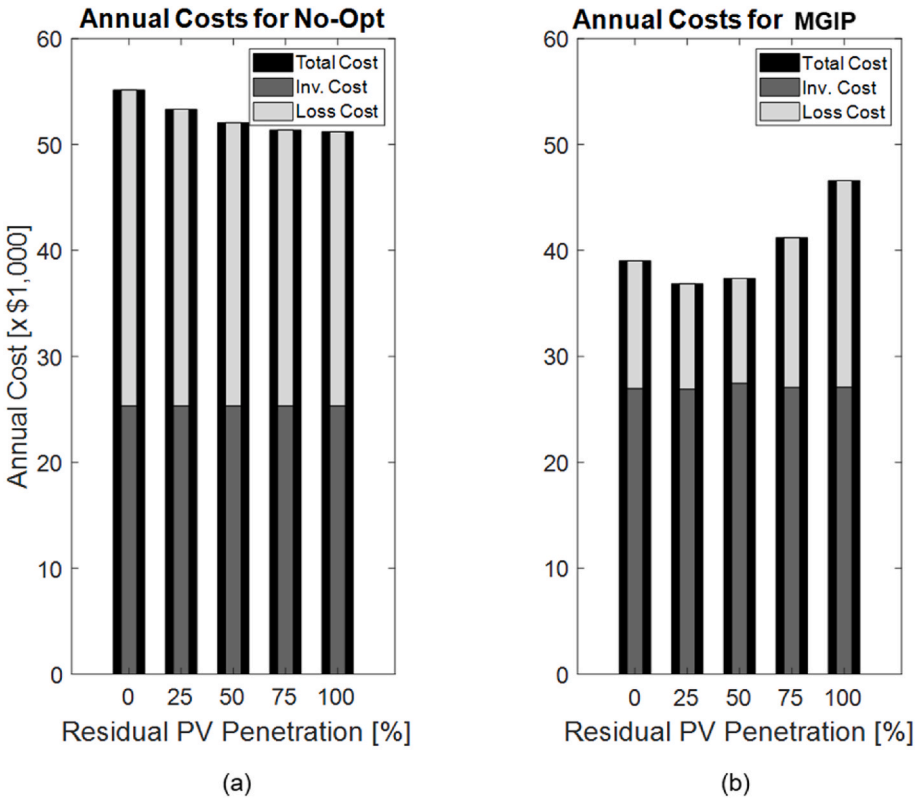

Fig. 10. Breakdown of total annualized cost for the grid integration of a cluster of minigrids.

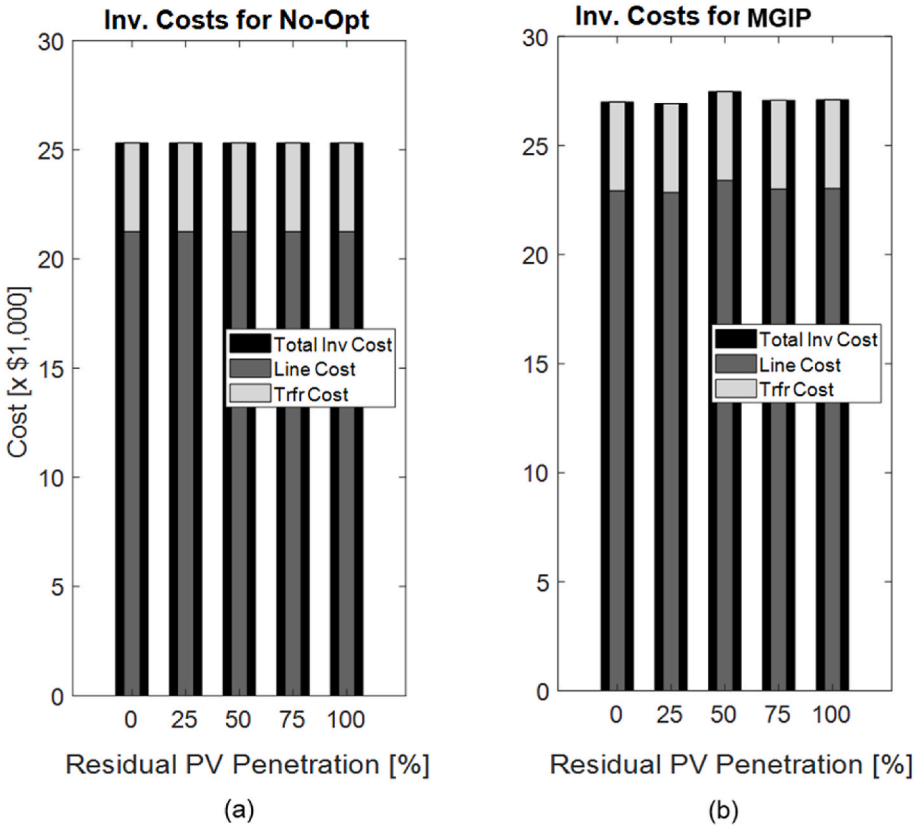

Fig. 11. Breakdown of investment cost for grid integration of cluster of minigrids.

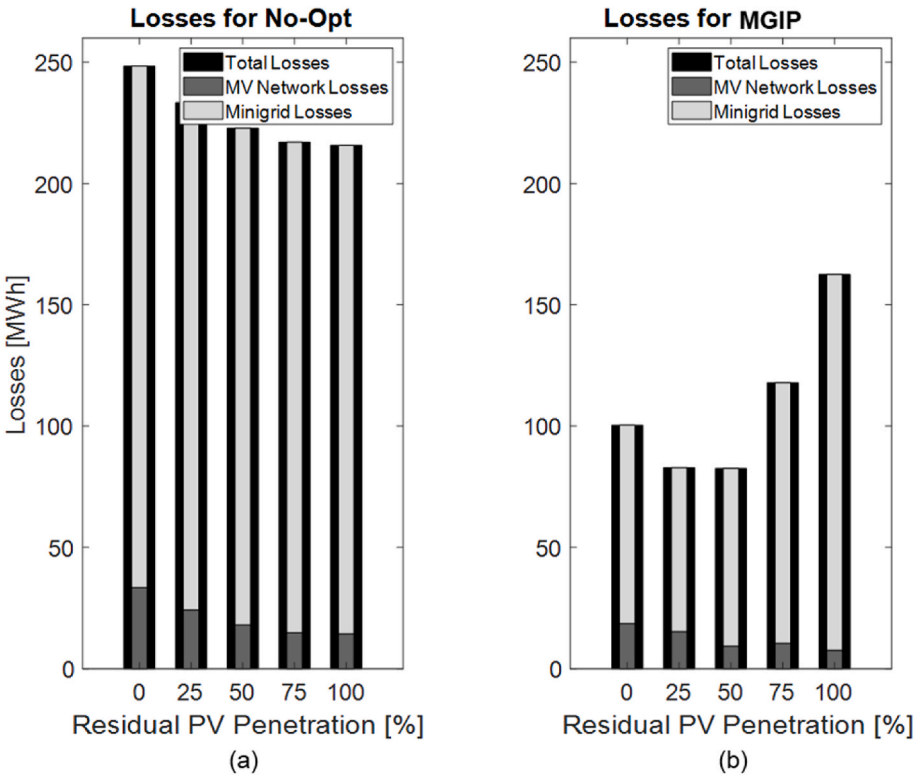

Fig. 12. Breakdown of annual losses.

minigrids is an important component of the analysis, it does not significantly drive the optimization solution as the losses component discussed hereafter.

Fig. 12 shows the total and breakdown of annual energy losses for the case study under consideration. Compared to No-Opt in Fig. 12(a), at its best scenario (25% PV penetration), the MGIP method in Fig. 12(b) leads to an annual energy saving of 150 MWh. This saving is enough to meet the Tier 4 yearly energy needs of 120 households, with an average

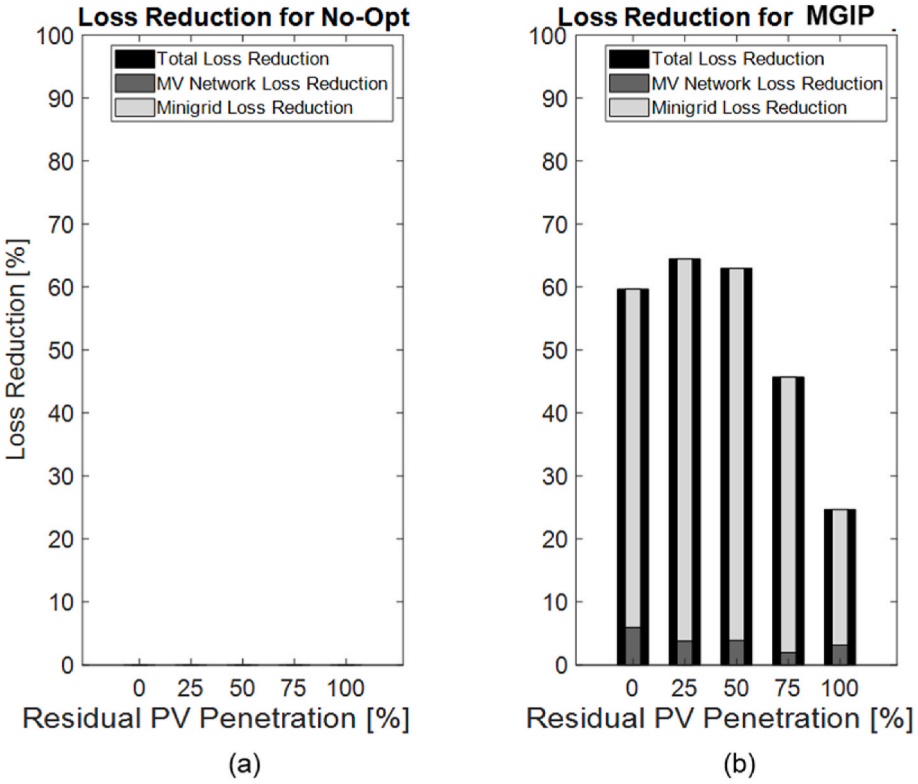

Fig. 13. Loss reduction potential.

consumption of 1250 kWh per annum [10]. Another way to demonstrate the value of the saved 150 MWh is to consider that the average annual electricity consumption per capita in Malawi (2019) is 108 kWh [46], meaning an additional 150 MWh on Malawi's grid could meet the needs of approximately 1388 people. With the World Bank predicting the deployment of over two hundred thousand solar PV minigrids by 2030, most of which will be in SSA [15], loss reduction benefits, such as those offered by MGIP should be carefully considered. Extrapolating the levels of loss reduction presented in this case study of 12 minigrids, the grid integration of 200,000 minigrid could lead to potential annual loss reduction of up to 2500 GWh. The magnitude of the loss reduction benefits will, of course, depend on the size of the minigrid, demand and demand profiles within the minigrid, and residual DERs in the minigrid.

As stated previously, Fig. 12 shows that the losses in the No-Opt method reduce with increasing residual generation capacity while for the MGIP methods, the losses go down and then up with an increasing PV penetration. This is so because the presence of local generation affects the power flow and voltages in the network. When the generation and grid infeed are collocated, the generator only affects the powerflow in the MV network and voltage in the minigrid networks in the No-Opt method. That is why the loss reduction increases with the increasing residual PV capacity. However, for MGIP, the grid infeed is not collocated with the residual PV; hence besides boosting the voltage, the capacity of the PV affects both MV and LV power flows, which affect losses. Although high losses are noted in the MGIP for the 100% residual PV penetration, they are still better compared to the No-Opt in Fig. 12(a), albeit with a small margin. The reduced impact of the MGIP for high PV penetration can be mitigated by incorporating storage to shift some of the high PV output into the evening peak.

Fig. 13(b) shows the loss reduction potential in the MGIP method as a percentage of losses in the No-Opt. The results show that for the case study modelled here, the MGIP method has a maximum loss reduction potential of 65% and a minimum of 25%, depending on the penetration of the residual DERs. The MGIP loss reduction benefits reported here are substantial compared to the 0% loss reduction potential for No-Opt method because when the main grid is integrated at the minigrid generator hub, the loss profile of the minigrid remains unaltered. Since the power networks in SSA are reportedly experiencing high network losses [2], it is important for future grid integration of minigrids not to compound the problem but to lessen it. MGIP method provides significant potential to achieve that.

Therefore, planning the grid integration of any cluster of minigrid using the method proposed in this paper will lead to slightly higher investment in network expansion but a better return on the cost of losses. Since electricity network efficiency is one of the issues in emerging countries, the MGIP method will be best placed to take advantage of existing offgrid infrastructure to achieve network efficiency in post-SDG7 distribution systems in developing countries. Depending on the size and type of incumbent minigrid DER, this efficiency will be realized in both the local minigrid networks and the interconnecting MV feeders.

5.2.3. *Network voltage profile improvement*

Although the voltage is not explicitly modelled as part of the objective function (1), the MGIP method leads to an improved voltage profile compared to No-Opt, as shown in Fig. 14. This should be expected for several reasons. Firstly, the MGIP method has voltage constraints (11) applied to both MV and LV nodes compared to the lack of constraints for No-Opt. Secondly, previous studies in distribution network planning have demonstrated that voltage improvement and loss reduction are positively correlated; hence the better loss performance

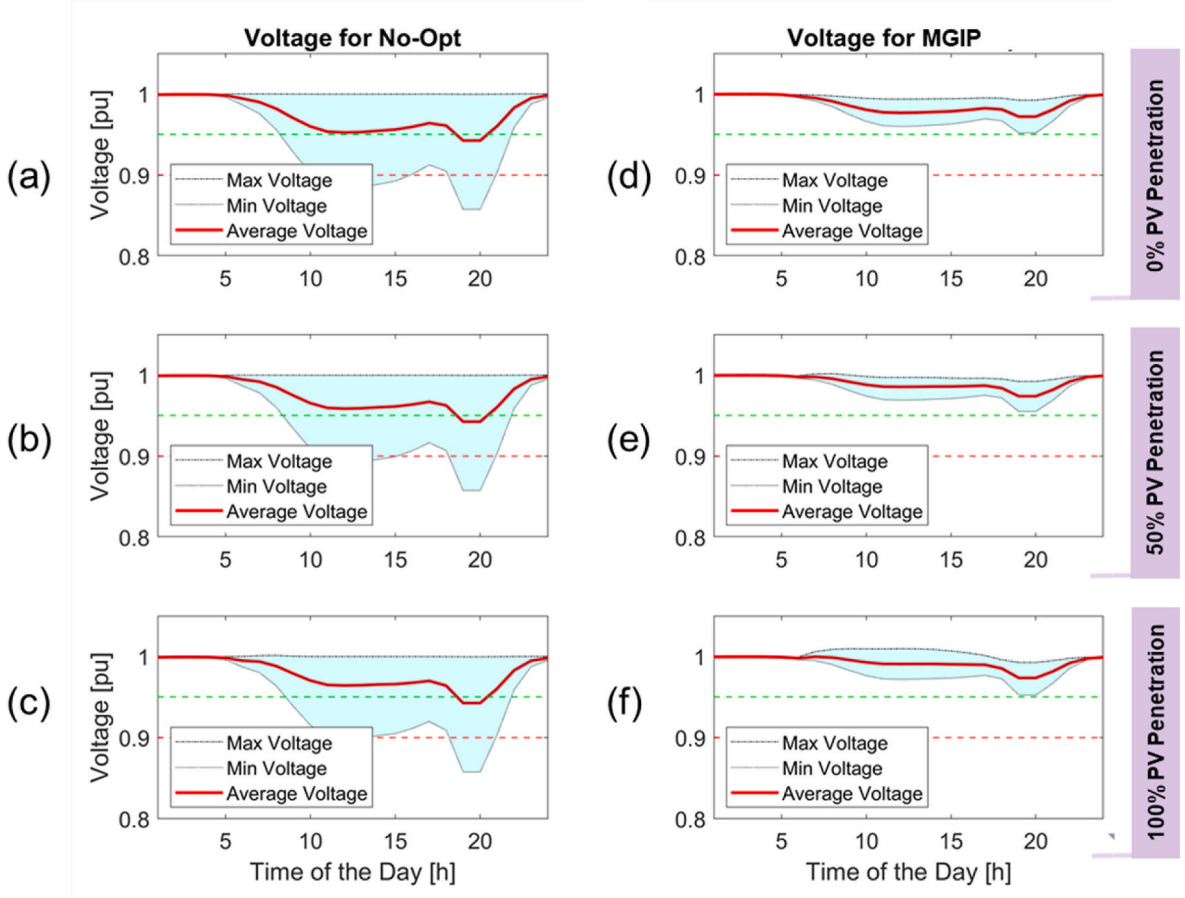

Fig. 14. Post grid integration voltage profiles (with 0, 50 and 100% PV).

for the MGIP should consequently result in a better voltage performance.

Fig. 14(a)–(c) shows significant undervoltage for No-Opt and no violations in the voltages for MGIP reported in Fig. 14(d)–(f). The base voltage in the case study was set to reflect the low quality of supply associated with most developing countries. Hence, No-Opt, which does not influence the magnitudes of power flows in the minigrid, leads to voltages below the strict lower limit of 0.95pu and the relaxed one of 0.9pu. Despite the increasing presence of PV during daytime (06:00 to 18:00), the voltage profile in the No-Opt method does not improve significantly as the generator and the grid infeed point are collocated.

However, the situation is different for both MGIP method which improves voltage profiles by the combination of the availability of local generation and different grid infeed points from the location of the local generators. Impact of the local generators can be observed in Fig. 14(f) where, unlike in the No-Opt method, during the daytime, there is no voltage breach, and the maximum voltages swell slightly above 1pu during the day for MGIP. The effect of point of grid infeed is felt in the evening peak when the PV is not available. Here, the voltages in Fig. 14 (d)–(f) record a moderate voltage trough around 19:00 while this trough is very big for No-opt in Fig. 14(a)–(c).

These results on voltages reveal a possible further saving on investment cost through the MGIP method. Since No-opt leads to voltage breaches, to achieve an acceptable quality of supply and accommodate load growth, minigrid network upgrades would be required during grid integration. It is debatable whether this would be affordable or a priority for the minigrid operator, leading to sustained power quality issues for customers even after attaining a grid connection. High voltage drops are associated with high network losses, and an increase in (LV) investment for No-opt would improve their losses. Regardless, the MGIP method achieves acceptable voltages with associated lower losses without any additional network reinforcement.

6. Conclusions and future work

This paper has proposed, formulated and tested a novel method appropriate for systematically planning the grid integration of minigrids (whether single or a cluster of minigrids) in developing countries. The need for the methodology has been shown by demonstrating that existing methods do not maximise the benefits of grid integration of minigrids, a new challenge in developing countries as further grid extension beyond achieving electricity access converges with offgrid electrification strategies. The formulation employs power systems analysis and distribution network planning techniques to jointly optimize mini-grid parameters, by identifying points of grid infeed points for each minigrid network, and MV reticulation and investments for the integration. Upon testing the proposed method on the grid integration of a single minigrid and a cluster of minigrid akin to those in developing countries, the method yields superior results compared to the existing practice of connecting the incoming grid as close as possible to the minigrid generator. Solutions from the proposed method have demonstrated that the MGIP method leads to significant loss reduction and voltage profile improvement, which outweigh the slightly higher investment cost which may be associated with the method.

The proposed method can be used by network planners to ensure optimality in the grid integration of minigrids in developing countries beyond energy access. Such application will help alleviate network efficiency and power quality challenges that characterize current energy access effects in main grids and minigrids in developing countries. On a larger scale, the significant optimal loss reduction associated with the MGIP method can free useable energy for other consumers as well as reducing the impact of minigrid integration on grid-wide load growth. Furthermore, the improvement of voltages compared to the No-Opt method signifies a major saving in the investment that may be required at the minigrid network level to improve the voltage profile of the grid integrated minigrids.

The MGIP method proposed here has demonstrated the value of systematically optimizing the grid integration of minigrids beyond achieving energy access in developing countries. This work is based on the premise that the minigrid is grid compatible and a prior decision has already been made to integrate it to the main grid. However, not all minigrids have the same level of grid compatibility and the benefits from grid integration using MGIP will have to be discounted by the cost of making such minigrids grid ready. Also, the presented method assumes that straight lines segments of the MV network connecting the minigrids can be used. Whereas operationally, the routing of these lines would be affected by local conditions in the topography such as terrain or elevation or the presence of protected areas. Another limitation of the presented method is that it uses deterministic data and a less efficient optimization technique. Future advancement of this work shall include the use of operational minigrid and the consideration of local obstacles to the reticulation of the MV lines, application of probabilistic methods to cover a wide range of operating conditions and the use of more efficient optimization techniques for evaluating this problem at a regional or country-level scale.

Declaration of competing interest

The authors declare that they have no known competing financial interests or personal relationships that could have appeared to influence the work reported in this paper.

Acknowledgements

This research has been carried out under a PhD Studentship supported by Scottish Funding Council and the University of Strathclyde.

References

[1] United Nations Department of Economic and Social Affairs, The Sustainable Development Goals Report 2018, UN, 2018.
[2] IEA, “Africa, Energy Outlook 2019, Paris, 2019 [Online]. Available: https://www.iea.org/reports/africa-energy-outlook-2019#energy-access%0Ahttps://www.iea.org/reports/africa-energy-outlook-2019%23africa-case.
[3] IEA, IRENA, UNSD, World Bank, WHO, Tracking SDG 7: the Energy Progress Report 2021, 2021. Washington DC.
[4] Vivid Economics; ARUP, Opportunities to Enhance Electricity Network Efficiency, 2015. London.
[5] C. Trimble, M. Kojima, I. Perez Arroyo, F. Mohammadzadeh, Financial Viability of Electricity Sectors in Sub-saharan Africa: Quasi-Fiscal Deficits and Hidden Costs, World Bank, Washington, DC, 2016.
[6] V. Jacome, N. Klugman, C. Wolfram, B. Grunfeld, D. Callaway, I. Ray, Power quality and modern energy for all, Proc. Natl. Acad. Sci. U.S.A. 116 (33) (2019) 16308–16313, https://doi.org/10.1073/pnas.1903610116.
[7] E. Day, Moving beyond Energy Access - the Challenge and Impact of Unreliable Electricity in Emerging Economies, 2020 [Online]. Available: https://www.energyeconomicgrowth.org/publication/eeg-energy-insight-moving-beyond-energy-access-challenge-and-impact-unreliable.
[8] J. Ayaburi, M. Bazilian, J. Kincer, T. Moss, Measuring ‘Reasonably Reliable’ access to electricity services, Electr. J. 33 (7) (2020), 106828, https://doi.org/10.1016/j.tej.2020.106828.
[9] M. Bhatia, N. Angelou, Beyond connections energy access redefined, ESMAP Technical Report (2015) 228, 008/15.
[10] H. Louie, Off-Grid Electrical Systems in Developing Countries, Springer International Publishing, Cham, 2018.
[11] O. Zinaman, et al., Power systems of the future, Electr. J. 28 (2) (Mar. 2015) 113–126, https://doi.org/10.1016/j.tej.2015.02.006.
[12] T. Levin, V.M. Thomas, Can developing countries leapfrog the centralized electrification paradigm? Energy Sustain. Dev. 31 (2016) 97–107, https://doi.org/10.1016/j.esd.2015.12.005.
[13] B. Tenenbaum, C. Greacen, T. Siyambalapitiya, J. Knuckles, From the Bottom up: How Small Power Producers and Mini-Grids Can Deliver Electrification and Renewable Energy in Africa, The World Bank, 2014.
[14] B. Tenenbaum, C. Greacen, D. Vaghela, Mini-Grids and Arrival of the Main Grid, World Bank, Washington, DC, 2018.
[15] Energy Sector Management Assistance Programme., W. B. Group, Mini Grids for Half a Billion People : Market Outlook and Handbook for Decision Makers, World Bank, Washington, DC, 2019 [Online]. Available: https://openknowledge.worldbank.org/handle/10986/31926.
[16] International Renewable Energy Agency (IRENA), Policies and Regulations for Renewable Mini-Grids, 2018 [Online]. Available: https://irena.org/-/media/Files/IRENA/Agency/Publication/2018/Oct/IRENA_mini-grid_policies_2018.pdf.

[17] S. Ackeby, J. Tjäder, C. Bastholm, The Role and Interaction of Microgrids and Centralized Grids in Developing Modern Power Systems, 2017 [Online]. Available: http://www.diva-portal.org/smash/record.jsf?pid=diva2:1180295.
[18] Nigerian Electricity Regulatory Commission (NERC), Regulations for Mini-Grid, 2016 [Online]. Available: https://nerc.gov.ng/index.php/component/remository/Regulations/NERC-Regulation-for-Mini-Grid/?Itemid=591.
[19] C. Greacen, R. Engel, T. Quetchenbach, A Guidebook on Grid Interconnection and Islanded Operation of Mini-Grid Power Systems up to 200kW, Lawrence Berkeley National Lab.(LBNL), Berkeley, CA (United States), California, 2013 [Online]. Available: https://publications.lbl.gov/islandora/object/ir%3A158819/datastream/PDF/view.
[20] Malawi Energy Regulatory Authority (MERA), Regulatory Framework for Minigrids, 2020 [Online]. Available: https://mera.mw/download/regulatory-framework-for-mini-grid-july-2020/?wpdmdl=1675&refresh=5ffd70a63a0151610444966.
[21] V. Kleftakis, D. Lagos, C. Papadimitriou, N.D. Hatziargyriou, Seamless transition between interconnected and islanded operation of DC microgrids, IEEE Trans. Smart Grid 10 (1) (2019) 248–256, https://doi.org/10.1109/tsg.2017.2737595.
[22] R. Majumder, M. Dewadasa, A. Ghosh, G. Ledwich, F. Zare, Control and protection of a microgrid connected to utility through back-to-back converters, Elec. Power Syst. Res. 81 (7) (2011) 1424–1435, https://doi.org/10.1016/j.epsr.2011.02.006.
[23] G.G. Talapur, H.M. Suryawanshi, L. Xu, A.B. Shitole, A reliable microgrid with seamless transition between grid connected and islanded mode for residential community with enhanced power quality, IEEE Trans. Ind. Appl. 54 (5) (2018) 5246–5255, https://doi.org/10.1109/tia.2018.2808482.
[24] P.S. Georgilakis, N.D. Hatziargyriou, Optimal distributed generation placement in power distribution networks: models, methods, and future research, IEEE Trans. Power Syst. 28 (3) (2013) 3420–3428, https://doi.org/10.1109/TPWRS.2012.2237043.
[25] M. Chikumbanje, D. Frame, S. Galloway, Enhancing Electricity Network Efficiency in Sub-saharan Africa through Optimal Integration of Minigrids and the Main Grid, in: 2020 IEEE PES/IAS PowerAfrica, PowerAfrica 2020, Aug. 2020, pp. 1–5, https://doi.org/10.1109/PowerAfrica49420.2020.9219976.
[26] M. Chikumbanje, D. Frame, S. Galloway, Minigrid integration in sub-Saharan Africaidentifying the 'optimal' point of connection, in: 2020 6th IEEE International Energy Conference (ENERGYCon), Sep. 2020, pp. 625–630, https://doi.org/10.1109/energycon48941.2020.9236457.
[27] C. Bastholm, F. Fiedler, Techno-economic study of the impact of blackouts on the viability of connecting an off-grid PV-diesel hybrid system in Tanzania to the national power grid, Energy Convers. Manag. 171 (2018) 647–658, https://doi.org/10.1016/j.enconman.2018.05.107.
[28] J. López, D. Pozo, J. Contreras, Static and dynamic convex distribution network expansion planning, in: Electric Distribution Network Planning, Springer, 2018, pp. 41–63.
[29] V. Vahidinasab, et al., Overview of electric energy distribution networks expansion planning, IEEE Access 8 (2020) 34750–34769, https://doi.org/10.1109/ACCESS.2020.2973455.
[30] H. Seifi, M.S. Sepasian, Electric Power System Planning, Springer, 2011.
[31] J.M. Gers, Distribution System Analysis and Automation, Institution of Engineering and Technology, London, 2013.
[32] P.C. Paiva, H.M. Khodr, J.A. Domínguez-Navarro, J.M. Yusta, A.J. Urdaneta, Integral planning of primary-secondary distribution systems using mixed integer linear programming, IEEE Trans. Power Syst. 20 (2) (2005) 1134–1143, https://doi.org/10.1109/TPWRS.2005.846108.
[33] G. Muñoz-Delgado, J. Contreras, J.M. Arroyo, Joint expansion planning of distributed generation and distribution networks, IEEE Trans. Power Syst. 30 (5) (2014) 2579–2590.
[34] I.J. Ramirez-Rosado, J.L. Bernal-Agustin, Genetic algorithms applied to the design of large power distribution systems, IEEE Trans. Power Syst. 13 (2) (1998) 696–703.
[35] A. Navarro-Espinosa, Low Carbon Technologies in Low Voltage Distribution Networks : Probabilistic Assessment of Impacts and Solutions, University of Manchester, 2015.
[36] K.P. Schneider, et al., Analytic considerations and design basis for the IEEE distribution test feeders, IEEE Trans. Power Syst. 33 (3) (May 2018) 3181–3188, https://doi.org/10.1109/TPWRS.2017.2760011.
[37] PES/IEEE, Resources PES Test Feeder, IEEE PES AMPS DSAS Test Feeder Working Group, 2020 accessed May 25, 2020, http://sites.ieee.org/pes-testfeeders/resources/.
[38] N.J. Williams, P. Jaramillo, B. Cornell, I. Lyons-Galante, E. Wynn, Load Characteristics of East African Microgrids, in: 2017 Ieee Pes Powerafrica Conf., 2017, pp. 236–241.
[39] Electricity Supply Corporation of Malawi (ESCOM), "Total Power Generation Output, ESCOM, Blantyre, Malawi, 2015.
[40] Millennium Challenge Account - Malawi (MCA-M), "ESCOM FINOP Project - Loss Study,", MCA-M, Lilongwe, 2015.
[41] S. Pfenninger, I. Staffell, Renewables.ninja, 2017 accessed Jul. 01, 2021, https://www.renewables.ninja/.
[42] R.C. Dugan, J.A. Taylor, D. Montenegro, Energy storage modeling for distribution planning, in: Papers Presented at the Annual Conference - Rural Electric Power Conference, May 2016, 2016-July, pp. 12–19, https://doi.org/10.1109/REPC.2016.11.
[43] World Bank, Malawi - Electricity Access Project, Washington DC, 2019 [Online]. Available: http://documents.worldbank.org/curated/en/520771561341715792/Malawi-Electricity-Access-Project.
[44] A.R. Inversin, Mini-grid Design Manual, Washington DC, 2000 [Online]. Available: http://documents.worldbank.org/curated/en/730361468739284428/Mini-grid-design-manual.
[45] L. Gonzalez-Sotres, C. Mateo Domingo, A. Sanchez-Miralles, M. Alvar Miro, Large-scale MV/LV transformer substation planning considering network costs and flexible area decomposition, IEEE Trans. Power Deliv. 28 (4) (2013) 2245–2253, https://doi.org/10.1109/tpwrd.2013.2258944.
[46] Our World in Data, Per capita electricity consumption, accessed Mar. 08, 2021, https://ourworldindata.org/grapher/per-capita-electricity-consumption?tab=chart&time=earliest..latest&country=~MWI.
[47] S.M. Ismael, S.H.E. Abdel Aleem, A.Y. Abdelaziz, A.F. Zobaa, State-of-the-art of hosting capacity in modern power systems with distributed generation, Renew. Energy 130 (2019) 1002–1020, https://doi.org/10.1016/j.renene.2018.07.008.